Journal of Sustainable Construction Materials and Technologies
Web page info: https://jscmt.yildiz.edu.tr
DOI: 10.47481/jscmt.1501001

JSCMT
Journal of Sustainable Construction Materials and Technologies

Research Article

Synergistic effects of GGBFS addition and oven drying on the physical and mechanical properties of fly ash-based geopolymer aggregates

Chereddy SONALI SRI DURGA[1], Chava VENKATESH*[1], Mukkala PRIYANKA[2], Bypaneni KRISHNA CHAITANYA[3], B. Naga Malleswara RAO[1], T. Muralidhara RAO[1]

[1]*Department of Civil Engineering, CVR College of Engineering, Vastunagar, Telangana, India*
[2]*Department of Civil Engineering, Malla Reddy Engineering College and Management Sciences, Telangana, India*
[3]*Department of Civil Engineering, R.V.R. & J.C. College of Engineering (A), Andhra Pradesh, India*

ARTICLE INFO

Article history
Received: 20 April 2024
Revised: 07 June 2024
Accepted: 10 June 2024

Key words:
Alkali activator solution, compressive strength, environmental impacts, geopolymer aggregates, water absorption

ABSTRACT

Conventional coarse aggregates, extracted from natural sources, pose environmental challenges such as habitat destruction, resource depletion, and high energy consumption. To mitigate these effects, this study prepared geopolymer aggregates (G.A.) using fly ash–GGBFS and an alkali activator solution through pelletization. Furthermore, two aggregate drying methods, oven drying, and ambient air drying, are adopted to evaluate their optimal performance through physical and mechanical tests. The results Indicated that oven-dried geopolymer aggregates exhibited optimal behavior in all experimental aspects compared to ambient air-dried aggregates. Specifically, the 80% fly ash–20% GGBFS mixed aggregates demonstrated lower crushing value (20.80%), impact value (24.7%), water absorption (13.67%), and abrasion values (7.01%) than other mixes. No considerable difference was observed in the density and specific gravity of aggregates between the two drying methods. Subsequently, these aggregates were used as a 100% replacement for conventional coarse aggregates in concrete, and the concrete's mechanical properties, such as compressive, split tensile, and flexural strengths, were investigated. Please update the following sentence in place of the highlighted sentence. The mix M3 (i.e., 80% fly ash–20% GGBFS mixed aggregates incorporated concrete) showed superior performance and are considered the optimum mix. Specifically, in the compressive strength results, the mix M3 showed a 26.31% and 14.28% strength increase compared to the 100% fly ash aggregates incorporated concrete mix in oven-dried aggregates and ambient-dried aggregates incorporated concrete, respectively. The linear regression equation derived from the experimental results was used to predict the split tensile and flexural strength, showing a good correlation between the experimental and expected results.

Cite this article as: Sonali Sri Durga, C., Venkatesh, C., Priyanka, M., Krishna Chaitanya, B., Rao, B. N. M., & Rao, T. M. (2024). Synergistic effects of GGBFS addition and oven drying on the physical and mechanical properties of fly ash-based geopolymer aggregates. *J Sustain Const Mater Technol*, 9(2), 93–105.

1. INTRODUCTION

Concrete, the most commonly used construction material, comprises aggregates and a cementitious matrix [1, 2]. The increasing demand for natural aggregates (N.A.) due to the rapid growth of the construction industry in the twenty-first century has significantly strained the environment [3]. To address this issue, researchers have been working on developing sustainable alternatives to natural aggregates for concrete production. These alternative aggregates can help conserve natural resourc-

***Corresponding author.**
*E-mail address: chvenky288@gmail.com

es, reduce the need for landfills by utilizing industrial and urban waste products, and contribute to a more sustainable built environment. A variety of grain-like solid wastes, such as recycled aggregates [4], waste glass [5], and steel slag [6], have been successfully used as alternative aggregates in concrete. As research on these grain-like solid wastes has advanced, there has been a growing interest in transforming powder-like solid wastes into grain-like artificial aggregates [7, 8].

Artificial aggregate technology offers a promising solution to two major problems: the excessive excavation of natural rock sources and the accumulation of waste materials [9]. This technology involves binding powder-like materials together and allowing them to harden, resulting in the formation of grain-like materials with desired aggregate sizes [10]. Among the various types of lightweight aggregates, sintered fly ash aggregates and cold-bonded cement-based aggregates have shown superior performance. However, the sintering method requires high temperatures ranging from 1000 °C to 1200 °C, which results in significant energy consumption and CO_2 emissions during the production of solid and lightweight aggregates [11, 12]. In contrast, the cold-bonding technique requires temperatures below 100 °C, consuming minimal energy and producing no CO_2 emissions in the creation of aggregates [13].

The characteristics of artificial aggregates, including bulk density and specific gravity, are influenced by various factors such as the curing regime, binder content, sintering temperature, and grain size [14]. Typically, artificial aggregates exhibit a compacted bulk density below 2.0 g/cm^3 and a loose bulk density below 1.2 g/cm^3. Their oven-dry and saturated surface-dried specific gravity range from 1.10 to 2.0 and 1.51 to 2.25, respectively. These properties classify them as lightweight aggregates (L.W.A.) according to UNE-EN-13055-1 (2003) [15, 16]. Higher binder content and grain size increase specific gravity and bulk density, while sintering at higher temperatures (950 °C–1100 °C) decreases bulk density due to bloating, moisture removal, and combustion of organic materials [17]. Water absorption of artificial aggregates ranges from 0.7 to 32.8% for 24 hours of immersion, influencing concrete workability [18]. Increased binder content, sintering temperature and duration, NaOH molarity, and Na_2SiO_3 content reduce water absorption by creating a denser microstructure [19, 20]. Two-step pelletization also decreases porosity compared to single-step pelletization [17].

The crushing strength of aggregates depends on pelletization factors, curing regime and age, binder content, density, size, and shape. Higher binder content, curing age, pelletization duration, and accelerated curing improve crushing strength [21]. Smaller aggregates (4–12 mm) exhibit greater crushing strength than coarser ones due to lower porosity [17, 22]. Surface treatment with soluble glass or water glass enhances strength by promoting hydration and repairing surface cracks [23, 24]. Sintering temperature, raw material composition, and alkali activator addition also influence strength. Geopolymer aggregates demonstrate enhanced strength through heat and solution curing, with improvements observed in Na_2O content, Na_2SiO_3-NaOH ratio, fluid-binder ratio, and molarity [25]. The pelletized artificial aggregates exhibit sufficient impact and crushing strength to meet the standards for structural applications as outlined in I.S.: 2386 (Part IV)-1963 [26].

Lightweight concrete (L.W.C.) made with sintered or alkali-activated artificial aggregates can achieve performance comparable to normal-weight concrete (N.W.C.) [27]. The compressive strength of L.W.C. is significantly influenced by the properties of lightweight aggregates (L.W.A.), such as porosity, specific gravity, crushing strength, water absorption, particle size distribution [28], as well as mix design parameters and curing conditions [29, 30]. Mineral admixtures can enhance concrete's compressive strength through pozzolanic and densification effects [31, 32]. However, concrete with artificial aggregates may have lower compressive strength than N.W.C. due to the inferior properties of the aggregates [33]. Concrete with sintered aggregates exhibits higher strength than concrete with cold-bonded aggregates due to the latter's higher porosity and lower strength [34]. Surface treatment of aggregates can improve concrete's compressive strength by up to 30% [35].

Concrete's tensile strength is contingent upon various factors, including the paste matrix, interfacial transition zone (I.T.Z.), and the tensile properties of aggregates [36]. Longer curing durations and higher strengths of mortar and aggregates typically result in increased tensile strength [37]. However, augmenting the volume of artificial aggregates may lead to a decrease in tensile strength due to failures originating within the aggregates themselves. It's worth noting that concrete's tensile properties rely more on mortar properties than aggregates, as diametric tension tends to cause splitting [38]. Comparatively, lightweight aggregates (L.W.A.) possess smaller surface areas, less angular shapes, and lower surface roughness, potentially leading to weaker aggregate transition zones when compared to normal-weight aggregates (N.W.A.) [39]. The flexural properties of concrete mirror split tensile strength, with matrix densification and reduced volumes of artificial aggregates, improving flexural performance. In lightweight concrete (L.W.C.), flexural properties primarily hinge on mortar characteristics, with artificial aggregates contributing minimally to flexural bending resistance. For instance, an increased volume of mortar can compensate for decreased aggregate volume, resulting in a higher flexural elastic modulus during bending [40, 41].

In the context of the current research, geopolymer aggregates (G.P.A.s) have emerged as a notable choice among various artificial aggregate options, including sintered aggregates and cold-bonded cement-based aggregates. G.P.A.s are favored for their lack of cement, minimal energy requirements during production, and exceptional capability to immobilize heavy metals. The development of geopolymer aggregates offers several advantages over traditional artificial aggregates. Firstly, the output of G.P.A.s does not require the use of cement, which significantly contributes to greenhouse gas emissions. By eliminating the need for cement, G.P.A.s can help reduce the carbon footprint of the construction industry. Secondly, the production of G.P.A.s consumes less energy compared to other artificial aggregate types, such as sintered aggregates, which require high-temperature processing. This lower energy consumption further enhances the environmental sus-

Table 1. Chemical characteristics (weight (%)) and physical characteristics of binders

Material	Fe_2O_3*	CaO*	SiO_2*	Al_2O_3*	MgO*	Na_2O*	SO_3*	K_2O*	LOI*	Specific gravity	Specific surface (m^2/g)
Cement	3.12	65.15	21.47	4.16	1.97	0.63	1.96	1.01	0.53	3.10	1.2
Fly ash	4.56	3.87	58.23	26.05	1.21	0.41	1.16	0.87	3.64	2.39	5.12
GGBS	2.06	44.7	32.25	12.14	4.23	0.87	0.84	–	2.91	2.86	6

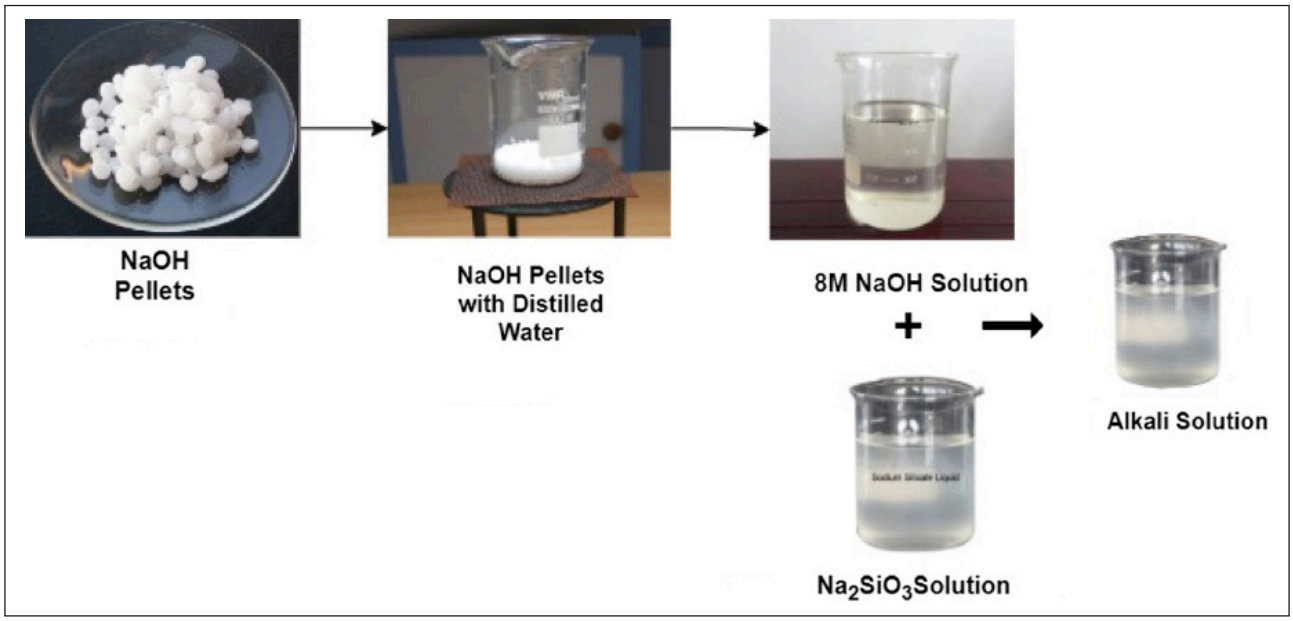

Figure 1. Preparation of Geopolymer/Alkali solution.

tainability of G.P.A.s. The drying method of the geopolymer aggregates plays a vital role in their physical and mechanical performance. Unfortunately, limited literature is available on the effect of drying methods on the mechanical and physical performance of G.P.A.s. Considering the research significance mentioned above, G.P.A.s were used as 100% replacement for the normal coarse aggregates in concrete, and their mechanical characteristics were evaluated. Furthermore, linear regression was performed using the experimental results, and prediction analysis was carried out using this equation.

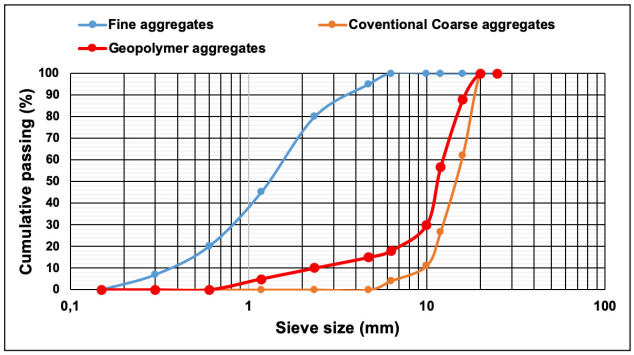

Figure 2. Grading curves of aggregates.

2. MATERIALS AND METHODS

2.1. Materials

The cement used in this study was Type I Ordinary Portland cement conforming to ASTM C150 [42]. It was procured from a local supplier, Mahashakthi Cement Dealers, in 50 kg bags. The chemical and physical properties of the cement, provided by the manufacturer, are presented in Table 1. Similarly, two Supplementary Cementitious Materials (S.C.M.s) were used as raw materials for geopolymer aggregates preparation - Class F fly ash, confirming to ASTM C618-22 [43], and ground granulated blast furnace slag (GGBFS), conforming to ASTM C989 [44]. The fly ash was procured from Vijayawada Thermal Power Plant, and the GGBFS was obtained from Visakhapatnam Steel Plant, both in 50 kg bags. Their chemical and physical compositions are provided in Table 1. The alkali activator solution was prepared in the laboratory by mixing analytical-grade sodium silicate (Na_2SiO_3) and 8M sodium hydroxide (NaOH) solutions in a 1:1.5 ratio, as shown in Figure 1, and was used as an adhesive. Moreover, the molar ratio of SiO_2/Na_2O in the sodium silicate solution is maintained at 2 (i.e., SiO_2/Na_2O=2). Locally available river sand and crushed granite stones were used as fine and coarse aggregates, respectively. The specific gravity, water absorption, gradation, and silt content were determined as per IS 383-2016 [45] and were within permissible limits. The sand had a specific gravity of 2.65, water absorption of 1%, and fineness modulus of 2.7. The coarse aggregate had a specific gravity of 2.8, water absorption of 0.5%, and sizes ranging between 4.75 mm and 20 mm. Figure 2 depicts the grading curve for aggregates.

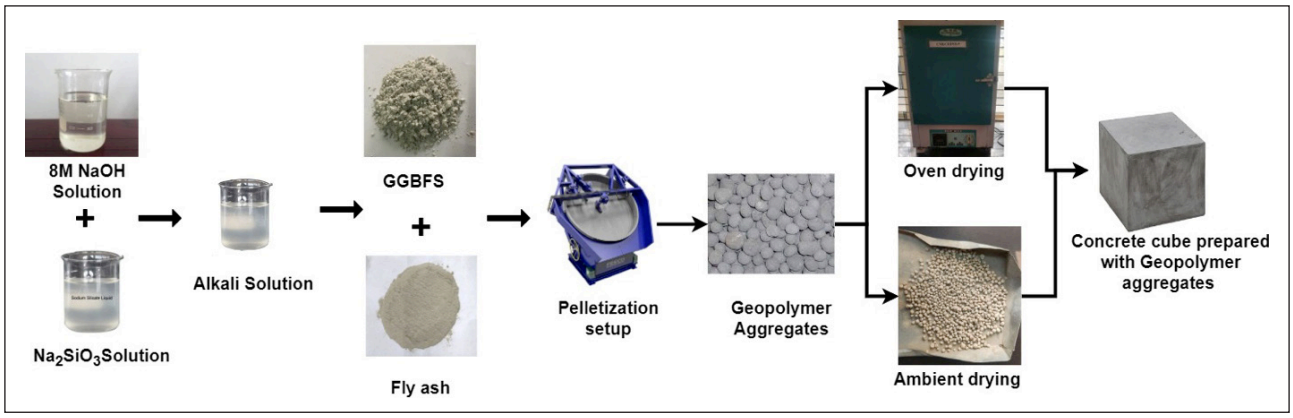

Figure 3. Preparation of Geopolymer aggregates

Table 2. Mix calculations for aggregates preparation (kg/m^3)

Aggregate mixes	Fly ash	GGBFS	NaOH	Na_2SiO_3	Geopolymer solution	The solution to binder ratio	Alkaline ratio ($NaOH/Na_2SiO_3$)	Molarity of geopolymer solution
100% FA	962	–	115.44	173.16	288.6	0.3	1:1.5	8
90% FA+10% GGBFS	865.8	96.2	115.44	173.16	288.6	0.3	1:1.5	8
80% FA+20 GGBFS	769.6	192.4	115.44	173.16	288.6	0.3	1:1.5	8

2.2. Experimental Methods

2.2.1. Pelletization

Geopolymer aggregates were manufactured utilizing a disc pelletizer set at a speed of 40 rotations per minute and an angle of tilt of 45°. A mixture of fly ash and GGBS was introduced into the pelletizer (Table 2), and the disc was rotated for 3 to 5 minutes before adding half of the solution to the binder. Rotation persisted for an additional 3 to 5 minutes. Throughout the pellet formation process, an alkaline solution was continuously sprayed onto the binder materials, facilitating accumulation [17]. Once the fresh pellets were formed, they underwent drying. Ambient-dried aggregates were exposed to standard atmospheric conditions at 25±2 °C.

In comparison, oven-dried aggregates were placed in an oven chamber set at 60 °C for 12 hours, then allowed to cool to ambient temperature. A schematic representation of the geopolymer aggregate production process is depicted in Figure 3. The resulting geopolymer aggregates exhibited a rounded shape, as shown in Figure 4. The efficiency of geopolymer aggregates is measured in terms of the weight percentage of aggregates retained on the 4.75 mm sieve [46]. In the present study, approximately 80% of the prepared geopolymer aggregates were retained on the 4.75 mm sieve. Hence, the efficiency of aggregate production is 80%. The following Eq.1 is used to calculate the efficiency of geopolymer aggregates.

Efficiency (η)=(weight of aggregates retained on the 4.75 mm sieve/total weight of aggregates produced)×100. (Eq.1)

2.2.2. Physical Tests on Aggregates

Aggregate Impact Value (A.I.V.), Aggregate Crushing Value (A.C.V.), and Aggregate Abrasion Value (AAV) are

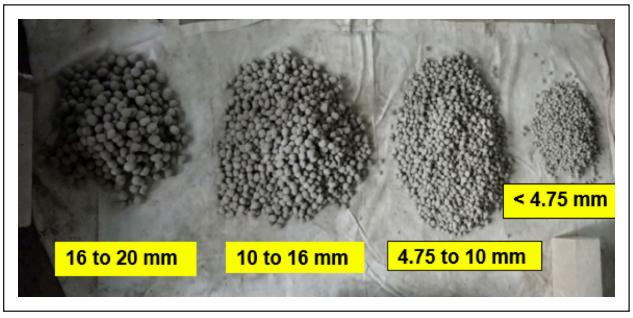

Figure 4. Geopolymer aggregates with rounded size.

measures of the resistance of an aggregate to crushing, impact, and abrasion, respectively, and are conducted as per I.S.: 2386 Part IV [47]. In the A.C.V. test, the aggregate sample is filled in a cylindrical steel mold and subjected to a compressive load of 40 tonnes for 10 minutes, and the percentage of crushed aggregate passing a 2.36 mm sieve is reported. In the A.I.V. test, the aggregate sample is subjected to blows from a hammer falling from a height of 380 mm, and the percentage of fine particles passing a 2.36 mm sieve is reported. In the AAV test, the aggregate sample is placed in an abrasion testing machine with steel balls and subjected to spinning, and the percentage of wear due to friction is reported. Specific Gravity, Bulk Density, and Water Absorption are measures of the density, weight per unit volume, and amount of water that an aggregate can absorb, respectively. They are conducted as per I.S.: 2386 Part III [48]. In the Specific Gravity test, the aggregate sample is dried, weighed, immersed in water, and weighed again. The ratio of the weight of a volume of aggregate to the weight of an equal volume of water is calculated. In the Bulk Density test, a cylindrical container is filled with an aggregate sample in three layers. Each layer is subjected to 25 strokes

Table 3. Mix calculations for concrete (kg/m^3)

Drying condition	Mix ID	Mix ID	Cement	Fine aggregate	Coarse aggregates	Geopolymer aggregate	Water	Water cement ratio
C.C.A.	Conventional coarse aggregates	CCA	425.32	596	835.64	–	191.39	0.45
Oven-dried	100% F.A.	M1	425.32	596	–	835.64	191.39	0.45
	90% FA+10% GGBFS	M2	425.32	596	–	835.64	191.39	0.45
	80% FA+20 GGBFS	M1	425.32	596	–	835.64	191.39	0.45
Ambient dried	100% F.A.	M1	425.32	596	–	835.64	191.39	0.45
	90% FA+10% GGBFS	M2	425.32	596	–	835.64	191.39	0.45
	80% FA+20 GGBFS	M3	425.32	596	–	835.64	191.39	0.45

from a tamping rod, and the mass of aggregates divided by the bulk volume is calculated. In the Water Absorption test, the oven-dried sample is immersed in water for 24 hours, removed, wiped, and weighed, and the increase in weight over dry weight divided by dry weight is expressed as water absorption.

2.2.3. Mix Calculations and Sample Preparation

Concrete cubes measuring 150 mm x 150 mm x 150 mm were prepared with a target 28-day compressive strength of 40 MPa as per mix design requirements, as shown in Table 3. The mix proportions and mixing methods followed IS 10262-2019 [49]. Cube specimens were demoulded after 24 hours and subjected to standard moist curing as per IS 516-1959 [50] in curing tanks at 27±2 °C for 7 and 28 days. For the experimental studies, a total of 210 samples were tested.

2.2.4. Compressive Strength

Compressive strength testing was conducted according to the specifications outlined in IS 516-1959 [50–52], utilizing a compression testing machine with a capacity of 2000 kN. The cubes underwent a cleaning process to remove any loose sand or particles, ensuring accuracy in the test results. Subsequently, they were positioned in the testing machine in a manner where the load was applied to the opposite sides of the 150 mm edge, and the axis of the specimen was meticulously aligned with the center of thrust. The load was then gradually applied at a steady rate of approximately 140 kg/cm2/min until failure occurred. Figure 5 provides a visual representation of the compressive strength test setup.

2.2.5. Split Tensile Strength

Concrete cylinders of 150mm diameter and 300mm height were prepared as per the mix proportions and curing method outlined in IS 516-1959 [50]. After 28 days of standard moist curing, the cylinders were tested for split tensile strength as per IS 5816 [53]. The cylinder specimen was placed horizontally between the loading surfaces of a 2000 kN capacity compression testing machine, and the load was applied without shock at a steady rate of 1.4 MPa/min. The alignment was adjusted so that the line of fracture was vertical and centered. The test was carried out until failure, and the maximum load at failure was recorded. Figure 6 illustrates the experimental photograph of the split tensile strength test.

Figure 5. Experimental photograph of compressive strength test.

2.2.6. Flexural Strength

For testing flexural strength, five beam specimens of 500 mm x 100 mm x 100 mm dimensions were prepared and moist cured for 28 days as per IS 516 [50–54]. The test procedure followed IS 516 specifications using a 200 kN capacity flexural testing machine. The beam was placed horizontally on rollers spaced 300 mm apart. Two point loads were applied at 180 mm center-to-center distance until failure occurred. Figure 7 illustrates the experimental photograph of the Flexural Strength Test—eq. 1 used to calculate the flexural strength of concrete.

Flexural strength (F_s)= PL/bd^2 Eq.1

P=Load applied to the beam at the two points (in Newtons, N)

Figure 6. Experimental photograph of Split tensile strength test.

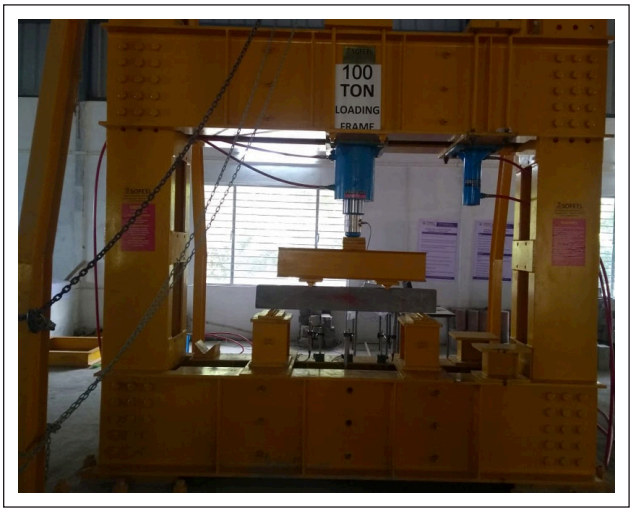

Figure 7. Experimental photograph of Flexural strength test.

L=Span length (distance between the supports) (in millimeters, mm)

b=Width of the specimen (in millimeters, mm)

d=Depth of the specimen (in millimeters, mm)

2.2.7. Linear Regression Analysis

In this study, linear regression analysis was used to determine the relationships between compressive strength, split tensile strength, and flexural strength [55, 56]. Using the derived equations, the split tensile and flexural strength values were predicted from the compressive strength data. These predicted values were then validated against the experimental results.

3. RESULTS AND DISCUSSION

3.1. Effect of GGBFS Addition and Drying Methods on Aggregate Properties

The aggregate crushing value was reduced from 25.84% to 20.8% for oven-dried and 29.5% to 26.04% for ambient air-dried mixes with 20% fly ash replacement by GGBFS (Table 4). The lowered fragmentation under compressive loads indicates improved aggregate strength and resistance capacity due to GGBFS incorporation [57–59]. This enhancement can be attributed to the higher reactivity of Ca-rich GGBFS, which promotes the formation of a dense and well-polymerized aluminosilicate gel network (as shown in Figure 8a), resulting in superior mechanical performance [17]. Similarly, the impact values decreased from 26.8% to 24.7% for oven-dried and 30.73% to 27.49% for ambient dried aggregates with 20% GGBFS addition. The drop in fine formation during sudden impact demonstrates better bonding of the aggregate matrix particles [60]. The abrasion values also followed a declining trend with GGBFS replacement due to improved cohesion. The water absorption substantially reduced from 10.39% to 7.01% for oven-dried and 14.52% to 10.61% for ambient dried aggregates as GGBFS was increased to 20%. The refined pores and discontinuities with the Ca-rich gel formation lead to lowered permeability and sorptivity [17]. The bulk density showed marginal improvements with denser aggregates. Overall, the addition of 20% GGBFS resulted in significant enhancements in strength, resistance to attrition, and durability properties of the fly ash-based geopolymer aggregates, meeting the I.S. code limits. This establishes the positive influence of GGBFS addition through the synergistic effects of Ca-rich gel formation.

Ambient air-dried aggregates showed inferior properties across all mix variations compared to oven-dried aggregates. The crushing, impact, and abrasion values were considerably higher for ambient dried aggregates. For example, the 80% fly ash - 20% GGBFS ambient dried mix exhibited 26.04% crushing compared to 20.8% for the oven-dried mix. This indicates additional microcrack formation from relatively slower moisture removal in ambient drying. Similarly, the water absorption of ambient-dried aggregates was higher, signifying increased porosity. The abrupt water evaporation in oven drying enables efficient moisture removal without damage to the aggregate structure.

On the contrary, ambient drying leads to weaker bonds by promoting shrinkage cracks. The specific gravity and density did not show any significant differences between oven-dried and ambient air-dried aggregates. However, the slower drying rate in ambient conditions ultimately affects the strength characteristics and resistance to fragmentation through microcrack development. In summary, oven drying

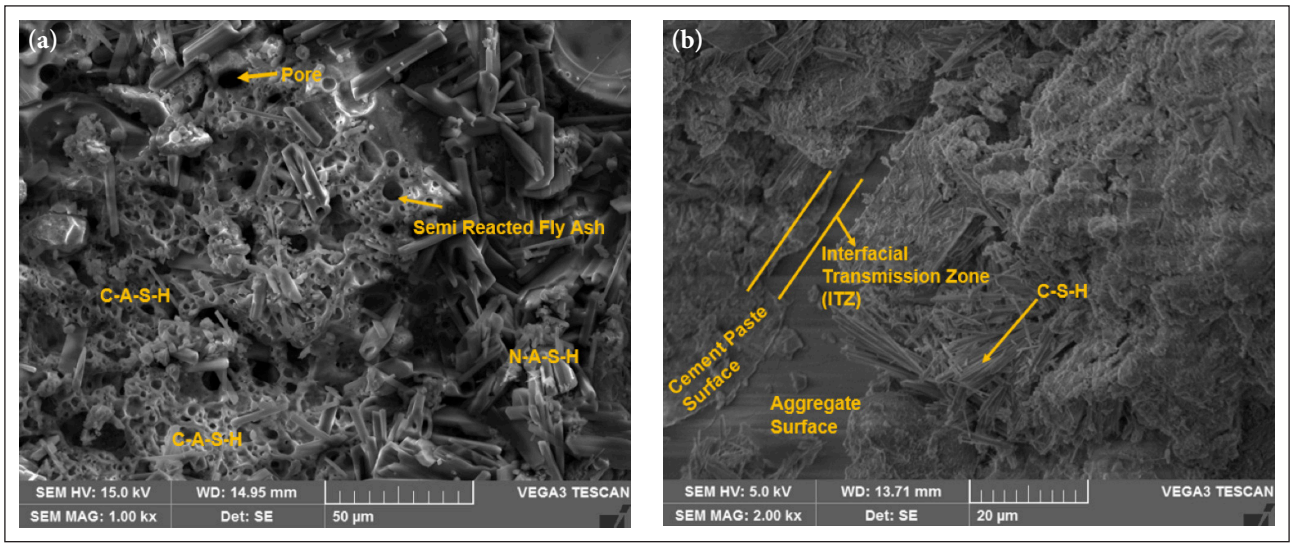

Figure 8. **(a)** S.E.M. of 80% F.A. + 20% oven-dried GGBFS geopolymer aggregates. **(b)** SEM of M3 concrete mix.

Table 4. Properties of aggregates

Test	CCA	IS 2386 limits	Oven dry			Ambient dry		
			M1	M2	M3	M1	M2	M3
Aggregate crushing value (%)	19.37	<30%	25.84	24.73	20.8	29.5	27.32	26.04
Aggregate impact value (%)	21.64	<30%	26.8	25.4	24.7	30.73	28.25	27.49
Abrasion value (%)	11.34	<3 0%	15.34	14.02	13.67	22.76	18.64	16.52
Water absorption (%)	5.34	<30%	10.39	8.46	7.01	14.52	13.05	10.61
Specific gravity	2.62	2.1–3.2	1.89	1.91	1.97	1.85	1.85	1.87
Bulk density (kg/m^3)	1556	1200–1750	962.30	969.36	969.52	961.42	964.31	958.27

enables rapid and uniform moisture removal without cracking, thereby showing consistently better properties over ambient air-drying for all aggregate mixes. The 80% fly ash - 20% GGBFS geopolymer aggregate mix with oven-drying methodology showed the most optimal performance.

3.2. Effect of GGBFS Addition and Drying Method on Compressive Strength

As evident from Figure 9, the compressive strength increased with higher GGBFS content in the geopolymer aggregate (G.A.) mixes for both oven-dried and ambient air-dried aggregates. The 80% fly ash - 20% GGBFS oven-dried Geopolymer aggregates incorporated concrete mix exhibited the maximum compressive strength of 44.64 MPa, showing 26.31% and 14.28% strength enhancements over the 100% fly ash G.A.s concrete for oven-dried and ambient dried samples respectively. The strength improvement is attributed to the higher reactivity of Ca-rich GGBFS, which promotes the formation of additional strength-contributing C-A-S-H gels along with the N-A-S-H gels from fly ash [61, 62]. The increased production of cementitious gel binds the aggregates strongly, contributing to superior load-bearing capacity. Moreover, The oven-dried G.A. incorporated concrete mixes have showed consistently higher compressive strengths over ambient air-dried G.A. concrete across all aggregate mixes. For instance, the concrete mix with 80%

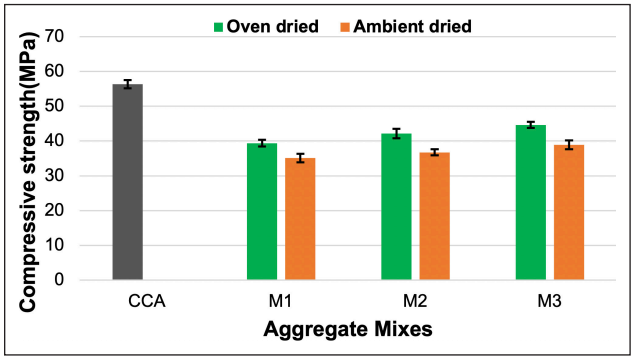

Figure 9. Compressive strength results.

fly ash and 20% GGBFS mixed aggregates had 13.3% greater strength in the oven-dried GA concrete mix compared to the ambient-dried GA concrete mix. This correlates to the denser aggregate structure from uniform, rapid oven drying, which translated to stronger interfacial transition zones (as shown in Figure 8b) and enhanced stress transfer efficiency in concrete [63].

In contrast, improper moisture removal during ambient air-drying could have led to weaker I.T.Z.s due to drying shrinkage. Slower drying also enables efflorescence formation, which increases porosity. Hence, as observed from the results, oven-dried G.A.s showed substantially better strength performance than ambient-dried G.A.s. In summary, GGBFS

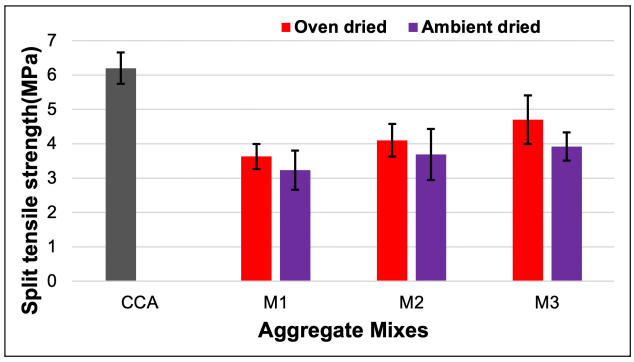

Figure 10. Split tensile strength result.

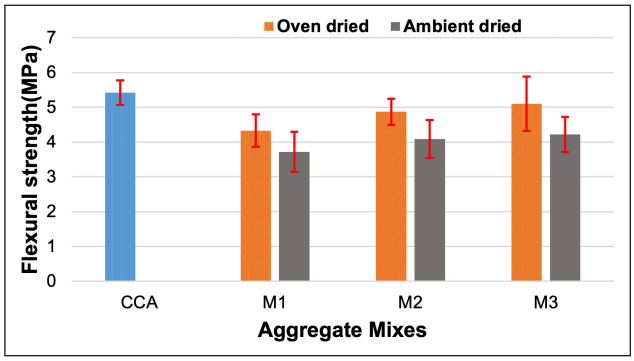

Figure 11. Flexural strength result.

addition enhances the compressive strength of G.A. concrete by promoting additional gel formation. At the same time, the oven drying method enables superior strength through a denser aggregate structure devoid of shrinkage cracks (as shown in Figure 8b). The 80% fly ash - 20% oven-dried GGBFS GA incorporated concrete mix showed the optimum results.

3.3. Effect of GGBFS Addition and Drying Method on Split Tensile Strength

As observed in Figure 10, the split tensile strength increased with higher GGBFS replacement in the geopolymer aggregate (G.A.) mixes, similar to the compressive strength trends. The concrete with 80% fly ash and 20% GGBFS mixed oven-dried aggregates exhibited a maximum split tensile strength of 4.7 MPa, showing enhancements of 29.46% and 21.67% over the 100% fly ash Geopolymer aggregates for the oven-dried and ambient air-dried aggregates, respectively. The greater production of cementitious C-A-S-H and N-A-S-H gels owing to GGBFS supplementation results in superior binding efficiency, which enables the concrete to resist better tensile cracking and opening of voids under the applied loads [61, 62]. This manifests as improved tensile strength. Moreover, the accelerator role of calcium facilitates geopolymerization, leading to refined microstructure and enhanced performance.

Additionally, oven-dried G.A. concrete showed consistently higher split tensile strengths over ambient air-dried G.A. concrete for all mixes. The 13–16% greater strength of oven-dried aggregates indicates the positive effects of controlled drying in facilitating stronger I.T.Z.s, allowing efficient transfer of stresses without crack propagation through

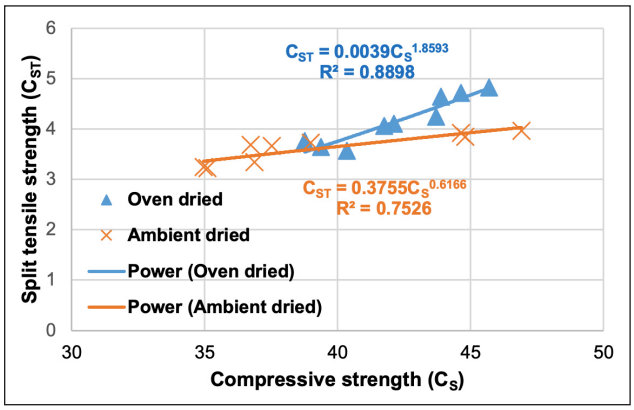

Figure 12. Regression analysis of compressive strength with split tensile strength.

the cross-section under tension [63]. In contrast, ambient drying leads to drying shrinkage cracks and poor bonding between aggregate and paste, lowering the tensile resistance [64]. The split tensile strength trends thus complement the compressive strength patterns, affirming the synergistic benefits of GGBFS incorporation and oven drying methodology in improving the strength attributes. The 80% fly ash - 20% GGBFS oven-dried G.A. demonstrated the optimal results meeting the target mean strength.

3.4. Effect of GGBFS Addition and Drying Method on Flexural Strength

The flexural strength increased from 4.33 MPa (Mix M1) to 5.1 MPa (Mix M3) for the oven-dried aggregates incorporated concrete mix and from 3.72 MPa to 4.22 MPa for the ambient air-dried geopolymer aggregate (GA) incorporated concrete mixes, as shown in Figure 11. The increment aligns with the formation of additional C-S-H gels (as shown in Figure 8b) owing to the higher reactivity of Ca-rich GGBFS, which enhances the load-bearing capacity [64]. As elucidated by Sitarz et al. [65], calcium modification disrupts aluminosilicate networks, facilitating increased dissolution and polycondensation, yielding semi-crystalline reaction products. This accelerated geopolymerization process aided by GGBFS produces a refined microstructure with superior inter-particle bonding strength, enabling enhanced resistance to bending stresses and cracks. Moreover, the release of Ca^{2+} ions further promotes the clay solubility and decomposition of mullite phases in fly ash, aiding better geopolymeric gel formation [66]. These synergistic effects facilitate notable improvements in flexural performance with GGBFS addition, as reflected in Figure 11.

The oven-dried G.A. concrete showed 12–15% higher flexural strength relative to ambient air-dried concrete across the different aggregate mixes (Fig. 11). The substantial enhancement highlights the significant impact of controlled drying in achieving consistent moisture removal without microcracking. This produces stronger transition zones between the aggregate and binder matrix (as shown in Figure 8b). Meanwhile, variable drying rates can induce stresses in ambient drying, causing shrinkage cracks that weaken the I.T.Z.s [63, 64]. Barbarey et al. [67] also reported a 10% drop in strength for ambient dried geopolymer

concrete compared to oven drying, which was attributed to cracking effects that influence flexural capacity.

3.5. Compressive Strength-Split Tensile Strength Correlation

A strong positive correlation (R^2=0.906) was obtained between the compressive and split tensile strength of geopolymer aggregates-based concrete prepared with varying GGBFS content and drying methods (Fig. 12). The split tensile strength increased concurrently from 3.63 MPa to 4.7 MPa as the compressive strength improved from 39.37 MPa to 44.64 MPa for oven-dried aggregates. The proportional enhancements are related to the comparable influences of GGBFS addition and controlled oven drying in refining the microstructure and paste-aggregate interfacial bonding [63]. The Ca-rich GGBFS promotes the dissolution of fly ash particles, aiding geopolymerization, which, along with the rapid, uniform drying, results in stronger transition zones between the two phases. This manifests as enhanced efficiency in transferring stresses under both compression and tension without crack initiation and propagation through the matrix [66]. Moreover, factors like the reduction in flaws and unreacted fly ash particles, which improve the compressive resistance by minimizing stress concentration sites, also raise the tensile strength by impeding crack propagation [68].

3.6. Compressive Strength-Flexural Strength Correlation

The compressive strength variations were also strongly correlated (R^2=0.898) with the flexural strength improvements between 3.72 MPa and 4.87 MPa for the geopolymer aggregates-based concrete (Fig. 13). The analogous effects of Ca-rich gel production from GGBFS and controlled oven drying in strengthening the paste matrix and aggregate interaction enhanced both capacities. The reduction in porosity refined the microstructure and improved inter-particle bonding while mitigating stress concentration sites. This mechanism simultaneously elevated the compressive and flexural strengths by delaying fracture under the respective loading scenarios. Additionally, the factors enhancing compressive resistance, like the decline in unreacted fly ash content and densification, aided superior flexural resistance by impeding crack initiation and propagation through the depth. Thus, the excellent correlation verifies that the strengthening mechanisms influencing both properties are interrelated.

3.7. Prediction of Split Tensile Strength

The experimental compressive strengths exhibited a strong linear correlation (R^2=0.906) with split tensile strengths for geopolymer aggregates incorporated concrete containing varying fly ash-GGBFS aggregate mixes and drying methods (Fig. 12). Leveraging this relationship, the regression equation derived was utilized to predict the split tensile strength values, which showed good agreement with experimental results, with variations within 1–3% (Table 5). For instance, the 100% fly ash based oven-dried geopolymer aggregates incorporated concrete showed only a 3.31% deviation between the experimental (3.63 MPa) and predicted (3.61 MPa) split tensile strengths. This concurrence verifies that the microstructural enhancements increasing the compressive strength, such as gel enrichment and reduced porosity, boost the tensile resistance by delaying crack initiation and propagation under tension loads. Additionally, factors like a refinement of flaws elevate the compressive capacity by minimizing stress concentration effects, and they raise the tensile strength simultaneously by impeding failure through the cross-section. Hence, a proportional increase in both strengths is obtained via similar strengthening mechanisms, as confirmed by the accurate prediction. The minor variations between experimental and predicted split tensile strengths for all oven-dried and ambient air-dried mixes substantiate the precision of the developed regression model for reliable forecasting based solely on the compressive strength data.

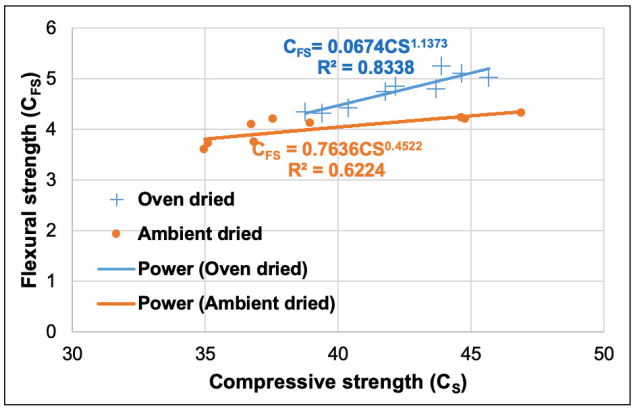

Figure 13. Regression analysis of compressive strength with flexural strength.

3.8. Prediction of Flexural Strength

The experimental relationship between compressive strength and flexural strength for the geopolymer aggregates incorporated concrete mixes (Fig. 13), represented by the linear regression equation, was utilized for anticipating flexural performance. As noted in Table 5, a good agreement was achieved between the experimental and predicted flexur-

Table 5. Predication of split tensile strength and flexural strength

Mixes	Experimental values						Predicted values			
	Oven-dried			Ambient dried			Oven-dried		Ambient dried	
	CS	ST	FS	CS	ST	FS	ST	FS	ST	FS
M1	39.37	3.63	5.42	35.11	3.23	3.72	3.61	4.39	3.37	3.82
M2	42.13	4.1	4.33	36.73	3.69	4.09	4.09	4.75	3.46	3.90
M3	44.64	4.7	4.87	38.94	3.92	4.22	4.55	5.07	3.59	4.00

al strengths with slight variations within 2–4%. This further verifies that the improvements in compressive strength from GGBFS-induced matrix densification and controlled oven drying can be correlated with concurrent flexural strength enhancements. The reduced porosity and enhanced paste-aggregate bonding enabled elevated resistance to bending stresses and fracture. Hence, the accurate prediction confirms that analogous mechanisms simultaneously elevate both capacities. Moreover, the precision substantiates the capability of the developed regression model for reliable flexural strength forecasting in geopolymer aggregate-based concretes using the easier-to-obtain compressive test data. This can enable quality assurance during mix design optimization for structural applications involving significant bending loads.

4. CONCLUSIONS

This study investigated the influence of GGBFS incorporation and drying methodology on the physical, mechanical, and microstructural characteristics of fly ash-based geopolymer aggregates and concrete. The following conclusions can be drawn:

- GGBFS addition (0% to 20%) to fly ash-based geopolymer aggregates significantly enhanced their properties: aggregate crushing value (25.84% to 20.8%), impact value (26.8% to 24.7%), abrasion value (15.34% to 13.67%), and water absorption (10.39% to 7.01%) for oven-dried mixes.
- Oven drying consistently resulted in superior aggregate properties compared to ambient air drying: crushing value (20.8% vs. 26.04%), impact value (24.7% vs. 27.49%), abrasion value (13.67% vs. 16.52%), and water absorption (7.01% vs. 10.61%) for 80% fly ash - 20% GGBFS mix.
- Compressive strength of geopolymer aggregate concrete increased with GGBFS content: 80% fly ash - 20% GGBFS oven-dried mix exhibited maximum strength (44.64 MPa), showing 26.31% and 14.28% enhancements over 100% fly ash mix for oven-dried and ambient dried samples, respectively.
- Split tensile and flexural strengths followed similar trends: 80% fly ash - 20% GGBFS oven-dried mix demonstrated optimal performance with 29.46% and 21.67% tensile strength enhancements and 12–15% higher flexural strength over ambient drying.
- Strong positive correlations between compressive strength and split tensile strength (R^2=0.906) and flexural strength (R^2=0.898) were observed, indicating simultaneous enhancement of mechanical properties.
- Regression equations accurately predicted split tensile (1–3% variation) and flexural strengths (2–4% variation) based on compressive strength data, substantiating the precision of the developed models for reliable forecasting.

In conclusion, the 80% fly ash - 20% GGBFS oven-dried geopolymer aggregate mix exhibited optimal physical, mechanical, and durability properties, with strong correlations enabling accurate performance predictions for structural applications. The findings establish that a controlled oven drying method and synergistic GGBFS addition can produce superior-quality fly ash-based geopolymer aggregates with reliable strength forecasting models.

ETHICS

There are no ethical issues with the publication of this manuscript.

DATA AVAILABILITY STATEMENT

The authors confirm that the data that supports the findings of this study are available within the article. Raw data that support the finding of this study are available from the corresponding author, upon reasonable request.

CONFLICT OF INTEREST

The authors declare that they have no conflict of interest.

FINANCIAL DISCLOSURE

The authors declared that this study has received no financial support.

USE OF AI FOR WRITING ASSISTANCE

Not declared.

PEER-REVIEW

Externally peer-reviewed.

REFERENCES

[1] Bagheri, S. M., Koushkbaghi, M., Mohseni, E., Koushkbaghi, S., & Tahmouresi, B. (2020). Evaluation of environment and economy viable recycling cement kiln dust for use in green concrete. *J Build Eng, 32*, 101809. [CrossRef]

[2] Venkatesh, C., Nerella, R., & Chand, M. S. R. (2021). Role of red mud as a cementing material in concrete: A comprehensive study on durability behavior. *Innov Infrastruct Solut, 6*(1), 13. [CrossRef]

[3] Xu, L. Y., Qian, L. P., Huang, B. T., & Dai, J. G. (2021). Development of artificial one-part geopolymer lightweight aggregates by crushing technique. *J Clean Prod, 315*, 128200. [CrossRef]

[4] Shivaprasad, K. N., Das, B. B., & Krishnadas, S. (2021). Effect of curing methods on the artificial production of fly ash aggregates. In *Recent Trends in Civil Eng: Select Proc of TMSF 2019* (pp. 23–32). Springer Singapore. [CrossRef]

[5] Harrison, E., Berenjian, A., & Seifan, M. (2020). Recycling of waste glass as aggregate in cement-based materials. Environ Sci Ecotechnol, 4, 100064. [CrossRef]

[6] Dong, Q., Wang, G., Chen, X., Tan, J., & Gu, X. (2021). Recycling of steel slag aggregate in portland cement concrete: An overview. *J Clean Prod, 282*, 124447. [CrossRef]

[7] Li, Z., Zhang, W., Jin, H., Fan, X., Liu, J., Xing, F., & Tang, L. (2023). Research on the durability and sustainability of an artificial lightweight aggregate concrete made from municipal solid waste incinerator bottom ash (MSWIBA). *Constr Build Mater, 365*, 129993. [CrossRef]

[8] Xu, L. Y., Huang, B. T., Lao, J. C., Yao, J., Li, V. C., & Dai, J. G. (2023). Tensile over-saturated cracking of Ultra-High-Strength Engineered Cementitious Composites (UHS-ECC) with artificial geopolymer aggregates. *Cem Concr Compos, 136*, 104896. [CrossRef]

[9] Tajra, F., Abd Elrahman, M., & Stephan, D. (2019). The production and properties of cold-bonded aggregate and its applications in concrete: A review. *Constr Build Mater, 225*, 29–43. [CrossRef]

[10] Qian, L. P., Xu, L. Y., Huang, B. T., & Dai, J. G. (2022). Pelletization and properties of artificial lightweight geopolymer aggregates (G.P.A.): One-part vs. two-part geopolymer techniques. *J Clean Prod, 374*, 133933. [CrossRef]

[11] Ma, X., Da, Y., He, T., Su, F., & Wan, Z. (2024). Improvement of harmlessness and resource utilization of incineration fly ash by high temperature sintering. *J Build Eng, 84*, 108589. [CrossRef]

[12] Biernacki, J. J., Vazrala, A. K., & Leimer, H. W. (2008). Sintering of a class F fly ash. *Fuel, 87*(6), 782–792. [CrossRef]

[13] Aungatichart, O., Nawaukkaratharnant, N., & Wasanapiarnpong, T. (2022). The potential use of cold-bonded lightweight aggregate derived from various types of biomass fly ash for preparation of lightweight concrete. *Mater Lett, 327*, 133019. [CrossRef]

[14] Huang, H., Yuan, Y., Zhang, W., & Gao, Z. (2019). Bond behavior between lightweight aggregate concrete and normal weight concrete based on splitting-tensile test. *Constr Build Mater, 209*, 306–314. [CrossRef]

[15] Kwek, S. Y., Awang, H., Cheah, C. B., & Mohamad, H. (2022). Development of sintered aggregate derived from POFA and silt for lightweight concrete. *J Build Eng, 49*, 104039. [CrossRef]

[16] UNE (2003). *Lightweight aggregates - Part 1: Lightweight aggregates for concrete, mortar, and grout*. UNE-EN-13055-1.

[17] Bekkeri, G. B., Shetty, K. K., & Nayak, G. (2023). Synthesis of artificial aggregates and their impact on performance of concrete: a review. *J Mater Cycles Waste Manag, 25*, 1–24. [CrossRef]

[18] Gomathi, P., & Sivakumar, A. (2014). Synthesis of geopolymer based class-F fly ash aggregates and its composite properties in concrete. *Arch Civ Eng, 60*(1), 55–75. [CrossRef]

[19] Vasugi, V., & Ramamurthy, K. (2014). Identification of admixture for pelletization and strength enhancement of sintered coal pond ash aggregate through statistically designed experiments. *Mater Des, 60*, 563–575. [CrossRef]

[20] Geetha, S., & Ramamurthy, K. (2013). Properties of geopolymerised low-calcium bottom ash aggregate cured at ambient temperature. *Cem Concr Compos, 43*, 20–30. [CrossRef]

[21] Asadizadeh, M., Clements, C., Hedayat, A., Tunstall, L., Gonzalez, J. A. V., Alvarado, J. W. V., & Neira, M. T. (2023). The effect of class F fly ash on the geopolymerization and compressive strength of lightweight aggregates made from alkali-activated mine tailings. *Constr Build Mater, 395*, 132275. [CrossRef]

[22] Colangelo, F., Messina, F., & Cioffi, R. (2015). Recycling of MSWI fly ash by means of cementitious double step cold bonding pelletization: Technological assessment for the production of lightweight artificial aggregates. *J Hazard Mater, 299*, 181–191. [CrossRef]

[23] Gomathi, P., & Sivakumar, A. (2015). Accelerated curing effects on the mechanical performance of cold bonded and sintered fly ash aggregate concrete. *Constr Build Mater, 77*, 276–287. [CrossRef]

[24] Gesoğlu, M., Özturan, T., & Güneyisi, E. (2007). Effects of fly ash properties on characteristics of cold-bonded fly ash lightweight aggregates. *Constr Build Mater, 21*(9), 1869–1878. [CrossRef]

[25] Qian, L. P., Huang, B. T., Xu, L. Y., & Dai, J. G. (2023). Concrete made with high-strength artificial geopolymer aggregates: Mechanical properties and failure mechanisms. *Constr Build Mater, 367*, 130318. [CrossRef]

[26] BIS. (1963). *Standard method of test for aggregates for concrete: Part IV Mechanical properties*. Bureau of Indian Standards, New Delhi. BIS I.S.: 2386 (Part IV)-1963.

[27] Terzić, A., Pezo, L., Mitić, V., & Radojević, Z. (2015). Artificial fly ash based aggregates properties influence on lightweight concrete performances. *Ceram Int, 41*(2), 2714–2726. [CrossRef]

[28] Mukkala, P., Venkatesh, C., & Habibunnisa, S. (2022). Evaluation of mix ratios of light weight concrete using geopolymer as binder. *Mater Today Proc, 52*, 2053–2056. [CrossRef]

[29] Gomathi, P., & Sivakumar, A. (2015). Accelerated curing effects on the mechanical performance of cold bonded and sintered fly ash aggregate concrete. *Constr Build Mater, 77*, 276–287. [CrossRef]

[30] Khanna, A. R., Satyanarayana, G. V. V., Raju, Y. K., & Ramanjaneyulu, N. (2023, September). Experimental investigation on mix design of foam concrete to fix ingredients for various densities. In A.I.P. *Conf Proc Vol. 2754*, No. 1. A.I.P. Publishing. [CrossRef]

[31] Venkatesh, C., Ruben, N., & Chand, M. S. R. (2020). Red mud as an additive in concrete: comprehensive characterization. *J Korean Ceram Soc, 57*(3), 281–289. [CrossRef]

[32] Venkatesh, C., Nerella, R., & Chand, M. S. R. (2020). Experimental investigation of strength, durability, and microstructure of red-mud concrete. *J Korean Ceram Soc, 57*(2), 167–174. [CrossRef]

[33] Ramanjaneyulu, N., Rao, M. S., & Desai, V. B. (2019). Behavior of self-compacting concrete partial replacement of coarse aggregate with pumice lightweight aggregate. *Int J Recent Technol Eng, 7*(6C2):434–440.

[34] Özkan, H., Kabay, N., & Miyan, N. (2022). Properties of cold-bonded and sintered aggregate using washing aggregate sludge and their incorporation in concrete: A promising material. *Sustainability, 14*(7), 4205. [CrossRef]

[35] Zhang, H., Zhao, Y., Meng, T., & Shah, S. P. (2016). Surface treatment on recycled coarse aggre-

gates with nanomaterials. *J Mater Civ Eng, 28*(2), 04015094. [CrossRef]

[36] Priyanka, M., Muniraj, K., & Madduru, S. R. C. (2022). Influence of geopolymer aggregates on micro-structural and durability characteristics of O.P.C. concrete. *J Build Pathol Rehabil, 7*(1), 13. [CrossRef]

[37] Strokova, V., Zhernovsky, I., Ogurtsova, Y., Maksakov, A., Kozhukhova, M., & Sobolev, K. (2014). Artificial aggregates based on granulated reactive silica powders. *Adv Powder Technol, 25*(3), 1076–1081. [CrossRef]

[38] Sahoo, S., & Selvaraju, A. K. (2020). Mechanical characterization of structural lightweight aggregate concrete made with sintered fly ash aggregates and synthetic fibres. *Cem Concr Compos, 113*, 103712. [CrossRef]

[39] Li, J., Niu, J., Wan, C., Liu, X., & Jin, Z. (2017). Comparison of flexural property between high performance polypropylene fiber reinforced lightweight aggregate concrete and steel fiber reinforced lightweight aggregate concrete. *Constr Build Mater, 157*, 729–736. [CrossRef]

[40] Punlert, S., Laoratanakul, P., Kongdee, R., & Suntako, R. (2017, September). Effect of lightweight aggregates prepared from fly ash on lightweight concrete performances. In *J Phys Conf Ser Vol. 901, No. 1, p. 012086*. I.O.P. Publishing. [CrossRef]

[41] Sravya, Y. L., Manoj, T., & Rao, M. S. (2021). Effect of temperature curing on lightweight expanded clay aggregate concrete. *Mater Today Proc, 38*, 3386–3391. [CrossRef]

[42] ASTM. (2019). *Standard specification for Portland cement. ASTM International, West Conshohocken*. ASTM C150, C150M-19a.

[43] ASTM. (2022). *Standard specification for coal FA and raw or calcined natural pozzolan for use in concrete*. ASTM International, West Conshohocken. ASTM C 618.

[44] ASTM. (2018). *Standard specification for slag cement for use in concrete and mortars*. ASTM International, West Conshohocken. ASTM C989, C989M-18a.

[45] BIS. (2016). *Specification for coarse and fine aggregates from natural sources for concrete*. Bureau of Indian Standards, New Delhi. BIS IS 383-2016.

[46] Shivaprasad, K. N., & Das, B. B. (2018). Determination of optimized geopolymerization factors on the properties of pelletized fly ash aggregates. *Constr Build Mater, 163*, 428–437. [CrossRef]

[47] BIS. (2002). *Part- IV Specification for methods of test for aggregates for concrete: Mechanical tests*. Bureau of Indian Standards, New Delhi. BIS IS 2386-2002.

[48] BIS. (2002). *Part- III Specification for methods of test for aggregates for concrete: Physical tests*. Bureau of Indian Standards, New Delhi. BIS IS 2386-2002.

[49] BIS. (2019). *Specification for mix design guidelines for concrete*. Bureau of Indian Standards, New Delhi. BIS IS 10262–2019.

[50] BIS. (1959). Specification for methods of tests for strength of concrete. Bureau of Indian Standards, New Delhi. BIS IS 516–1959.

[51] Chava, V., & Chereddy, S. S. D. (2023). Effect of calcination on the physical, chemical, morphological, and cementitious properties of red mud. *J Sustain Constr Mater Tech, 8*(4), 297–306. [CrossRef]

[52] Chava, V., Mv, S. R., Munugala, P. K., & Chereddy, S. S. D. (2024). Effect of mineral admixtures and curing regimes on properties of self-compacting concrete. *J Sustain Constr Mater Tech, 9*(1), 25–35. [CrossRef]

[53] BIS. (1999). *Specification for splitting tensile strength of concrete—method of test*. Bureau of Indian Standards, New Delhi. BIS IS 5816-1999.

[54] Durga, C. S. S., Venkatesh, C., Muralidhararao, T., & Bellum, R. R. (2023). Crack healing and flexural behaviour of self-healing concrete influenced by different bacillus species. *Res Eng Struct Mater, 9*(4), 1459–1475. [CrossRef]

[55] Ruben, N., Venkatesh, C., Durga, C. S. S., & Chand, M. S. R. (2021). Comprehensive study on performance of glass fibers-based concrete. *Innov Infrastruct Solut, 6*(2), 112. [CrossRef]

[56] Chaitanya, B. K., Sivakumar, I., Madhavi, Y., Cruze, D., Venkatesh, C., Naga Mahesh, Y., & Sri Durga, C. S. (2024). Microstructural and residual properties of self-compacting concrete containing waste copper slag as fine aggregate exposed to ambient and elevated temperatures. *Infrastructures, 9*(5), 85. [CrossRef]

[57] Li, Y., Huang, L., Gao, C., Mao, Z., & Qin, M. (2023). Workability and mechanical properties of GGBS-RFBP-FA ternary composite geopolymer concrete with recycled aggregates containing recycled fireclay brick aggregates. *Constr Build Mater, 392*, 131450. [CrossRef]

[58] Nicula, L. M., Manea, D. L., Simedru, D., Cadar, O., Ardelean, I., & Dragomir, M. L. (2023). The advantages of using GGBS and ACBFS aggregate to obtain an ecological road concrete. *Coatings, 13*(8), 1368. [CrossRef]

[59] Abdollahnejad, Z., Mastali, M., Woof, B., & Illikainen, M. (2020). High strength fiber reinforced one-part alkali activated slag/fly ash binders with ceramic aggregates: Microscopic analysis, mechanical properties, drying shrinkage, and freeze-thaw resistance. *Constr Build Mater, 241*, 118129. [CrossRef]

[60] Erdem, S., Dawson, A. R., & Thom, N. H. (2012). Influence of the micro- and nanoscale local mechanical properties of the interfacial transition zone on impact behavior of concrete made with different aggregates. *Cem Concr Res, 42*(2), 447–458. [CrossRef]

[61] Criado, M., Aperador, W., & Sobrados, I. (2016). Microstructural and mechanical properties of alkali activated Colombian raw materials. *Materials, 9*(3), 158. [CrossRef]

[62] Gao, X., Yu, Q. L., & Brouwers, H. J. H. (2016, August). Development of alkali activated slag-fly ash mortars: mix design and performance assessment. In *4th Int Conf Sustain Constr Mater Tech, SCMT 2016* (p. S167). [CrossRef]

[63] Elsharief, A., Cohen, M. D., & Olek, J. (2005). Influence of lightweight aggregate on the microstructure and durability of mortar. *Cem Concr Res, 35*(7), 1368–1376. [CrossRef]

[64] Abd Razak, R., Al Bakri, A. M., Kamarudin, H., Is-

mail, K. N., Hardjito, D., & Zarina, Y. (2016). Performances of Artificial Lightweight Geopolymer Aggregate (ALGA) in O.P.C. Concrete. *Key Eng Mater, 673*, 29–35. [CrossRef]

[65] Sitarz, M., Urban, M., & Hager, I. (2020). Rheology and mechanical properties of fly ash-based geopolymer mortars with ground granulated blast furnace slag addition. *Energies, 13*(10), 2639. [CrossRef]

[66] Bellum, R. R., Venkatesh, C., & Madduru, S. R. C. (2021). Influence of red mud on performance enhancement of fly ash-based geopolymer concrete. *Innov Infrastruct Solut, 6*(4), 215. [CrossRef]

[67] Barbarey, M. S., Seleman, M. M. E. S., El Kheshen, A. A., & Zawrah, M. F. (2024). Utilization of ladle furnace slag for fabrication of geopolymer: Its application as catalyst for biodiesel production. *Constr Build Mater, 411*, 134226. [CrossRef]

[68] Bellum, R. R., Al Khazaleh, M., Pilla, R. K., Choudhary, S., & Venkatesh, C. (2022). Effect of slag on strength, durability and microstructural characteristics of fly ash-based geopolymer concrete. *J Build Pathol Rehabil, 7*(1), 25. [CrossRef]